Electronic Supplemental Information

Tetraphenylethylene(TPE)-containing metal-organic nanobelt and its turn-on fluorescence for Sulfide (S^{2-})

Kaixiu Li,[†,#] Zhengguang Li,[†,#] Die Liu,[,‡] Mingzhao Chen,[‡] Shi-Cheng Wang,[§] Yi-Tsu Chan[§] and Pingshan Wang[*,†,‡]*

[†]Department of Organic and Polymer Chemistry; Hunan Key Laboratory of Micro & Nano Materials Interface Science, College of Chemistry and Chemical Engineering; Central South University, Changsha, Hunan 410083, China

E-mail: chem-ld@gzhu.edu.cn (D. Liu). chemwps@csu.edu.cn (P. Wang).

[‡]Institute of Environmental Research at Greater Bay Area; Key Laboratory for Water Quality and Conservation of the Pearl River Delta, Ministry of Education; Guangzhou Key Laboratory for Clean Energy and Materials; Guangzhou University, Guangzhou 510006, China

[§]Department of Chemistry, National Taiwan University, Number 1, Section 4, Roosevelt Road, Taipei 10617, Taiwan

Table of Contents

1. General Procedures

NMR spectra. NMR spectra were recorded on a Bruker ADVANCE 400 or 500 NMR Spectrometer. 1H NMR chemical shifts are reported in ppm downfield from tetramethylsilane (TMS) reference using the residual protonated solvent as an internal standard.

Mass spectra. Mass spectra of complexes and ligands were determined on Waters Synapt G2 Mass Spectrometer under the following conditions: ESI capillary voltage, 3.5 kV; cone voltage, 35 V; desolvation gas flow, 800 L/h. All chemicals were purchased from commercial suppliers and used without further purification unless otherwise specified.

Collision Cross-Sections Calibration. The calibration curve was established according to the protocol listed in the literature using published collision cross-sections S3 of polyalanine, cytochrome c (bovine), reserpine, lysozyme, and insulin (human).[S1] A plot of corrected drift times versus corrected cross-sections of calibrants fitted with power functions was used as a calibration curve for cross-section measurements.

UV-vis and emission spectral analysis. Absorption spectra were measured with Hitachi (model U-3010) UV-Vis spectrophotometer in a 1-cm quartz cell. Emission spectra were measured with Hitachi (F-7000) fluorescence spectrophotometer in a 1-cm quartz cell under the following conditions: EX Slit, 5.0 nm; EM Slit, 5.0 nm; PMT Voltage, 500 V for complex and EX Slit, 5.0 nm; EM Slit, 2.5 nm; PMT Voltage, 500 V for ligand.

Dynamic light scattering (DLS) experiments. Dynamic light scattering (DLS) was carried out on a Nano-ZS90 instrument at room temperature.

2. Synthesis and discussion of the related ligands and complexes

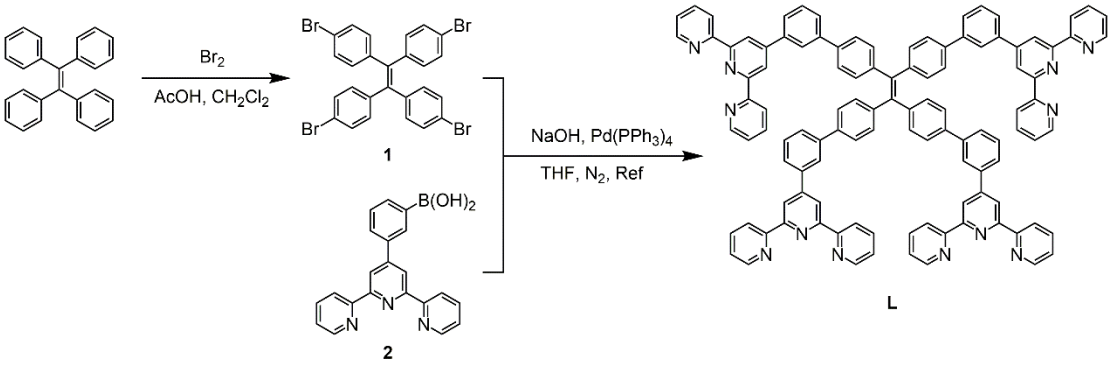

Scheme S1. Synthetic Route of ligand **L**.

Synthesis of compound **1**[S2]: Bromine (4 mL, 80 mmol) was added over a 5 min period to a solution of tetraphenylethylene (3.32 g, 10 mmol) in 30 mL of glacial acetic acid at 0 °C. After further adding dichloromethane (40 mL), the resulting mixture was heated at 50 °C for about 30 min [based on thin layer chromatography (TLC) detection]. The reaction mixture was added to 150 mL ice water, and the precipitated solid was filtered and washed repeatedly with water and ethanol and give compound **1** (5.90 g, 9.1 mmol) as a white solid in 91% yield. ^{1}H NMR (400 MHz, 298 K, $CDCl_3$, ppm) δ = 7.26 (d, *J* = 8.4 Hz, 8H), 6.84 (d, *J* = 8.4 Hz, 8H);

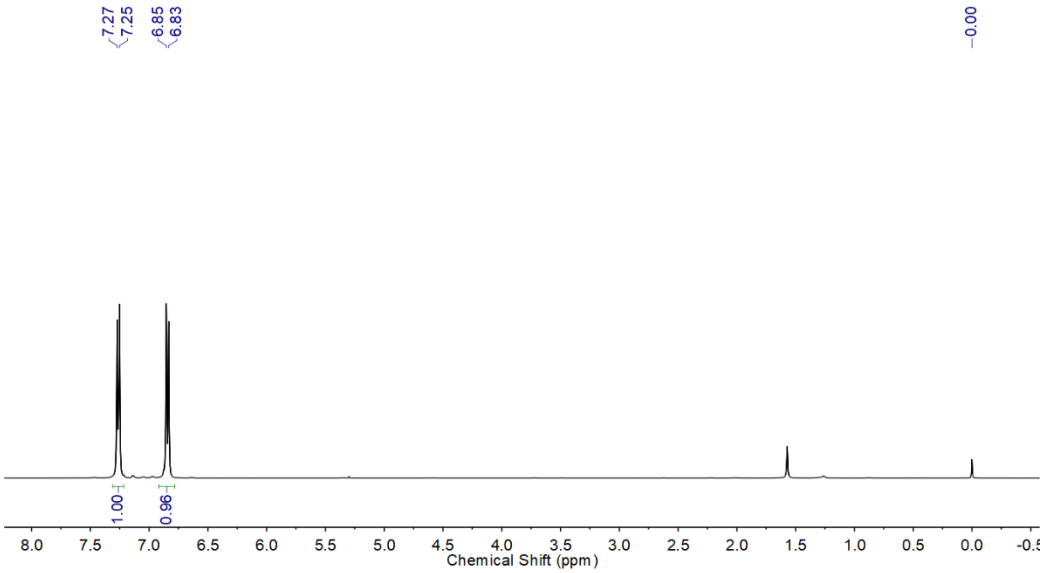

Figure S1. ^{1}H NMR spectrum of compound **1** in $CDCl_3$.

Synthesis of compound **L**: To a mixture of **1** (324 mg, 0.5 mmol) and 4'-(3-boronatophenyl) [2,2':6',2"] terpyridine (882 mg, 2.5 mmol) in THF (150 mL), aqueous NaOH (200 mg, 5 mmol, 1 M) was added. The system was pumped and backfilled with nitrogen; then $Pd(PPh_3)_4$ (142 mg, 0.12 mmol) was added. After refluxing for 48 h under nitrogen, the mixture was cooled to 25 °C and evaporated under reduced pressure. The residue was purified by flash column chromatography (Al_2O_3) eluting with CH_2Cl_2/CH_3OH ether and recrystallization with CH_2Cl_2/CH_3OH to give **L** (500 mg, 0.32 mmol) as a white solid in 64 yield; ^{1}H NMR (400 MHz, 298 K, $CDCl_3$, ppm): δ = 8.75 (s, 8H), 8.70-8.61 (m, 16H), 8.11 (s, 4H), 7.85 (td, *J* = 7.8, 1.8 Hz, 12H), 7.69 (d, *J* = 8.0 Hz, 4H), 7.58-7.50 (m, 12H), 7.33-7.29 (m, 16H); ^{13}C NMR (101 MHz, 298 K, $CDCl_3$, ppm): δ = 156.25, 155.93, 150.42, 149.12, 143.23, 141.66, 140.55, 139.01, 138.85, 136.84, 132.10, 129.29, 127.79, 126.83, 126.20, 126.00, 123.80, 121.37, 119.05; ESI-MS: calcd. for $C_{110}H_{72}N_{12}$. $[M+2H]^{2+}$: *m/z* = 781.809; found: 781.816.

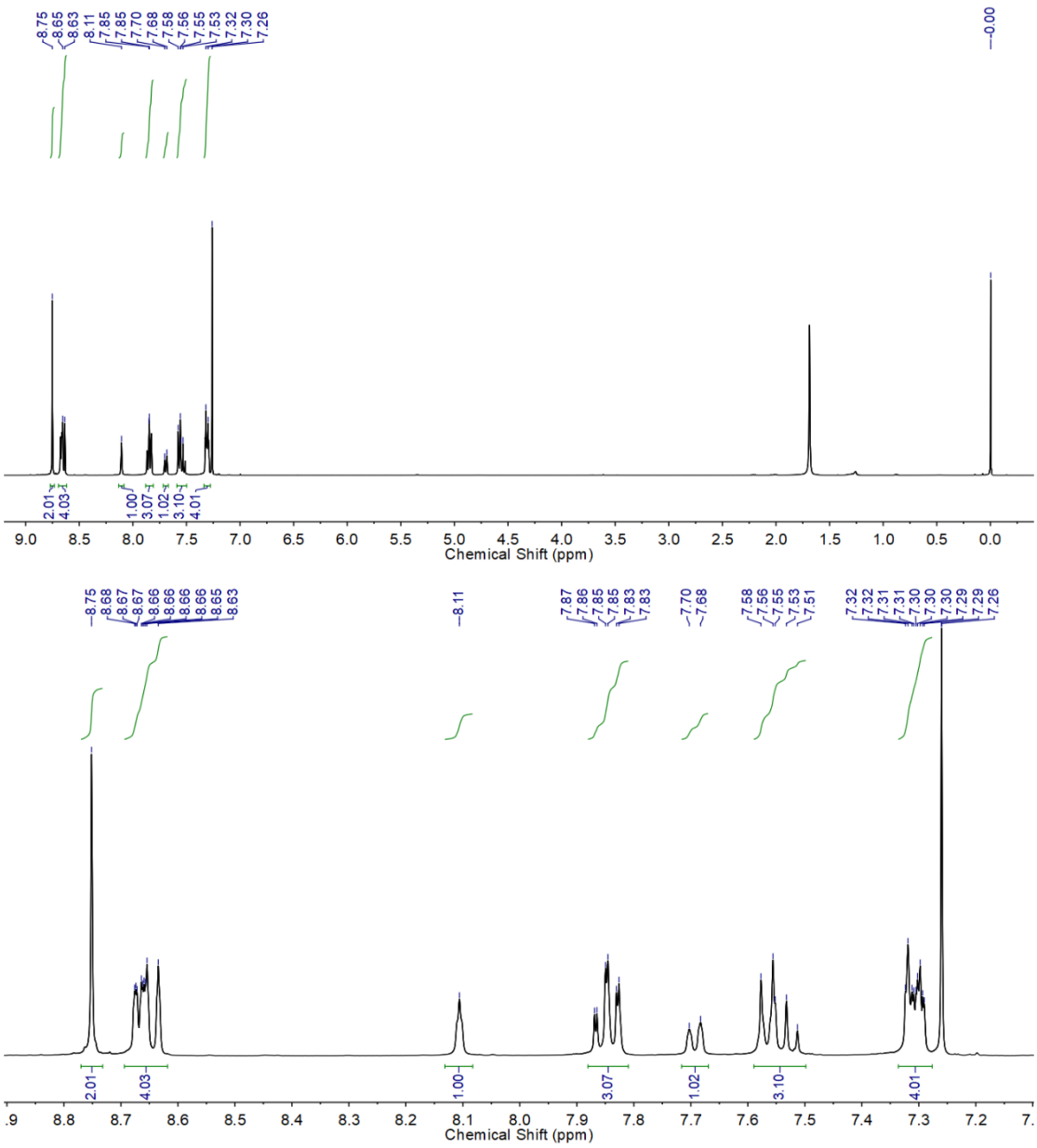

Figure S2. ^{1}H NMR spectrum of ligand **L** in $CDCl_3$.

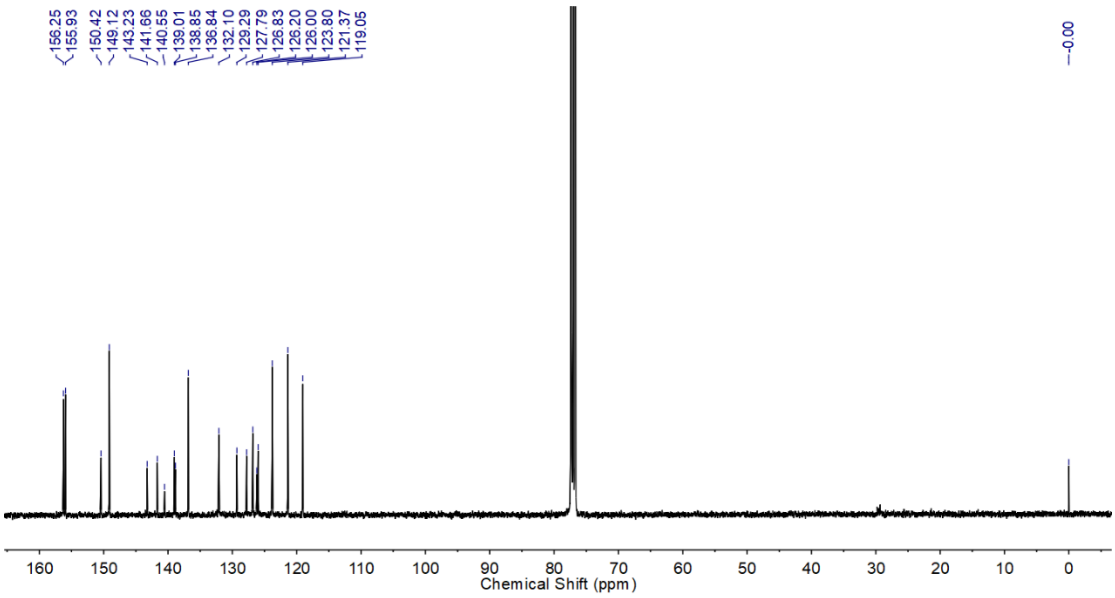

Figure S3. ^{13}C NMR spectrum of ligand **L** in $CDCl_3$.

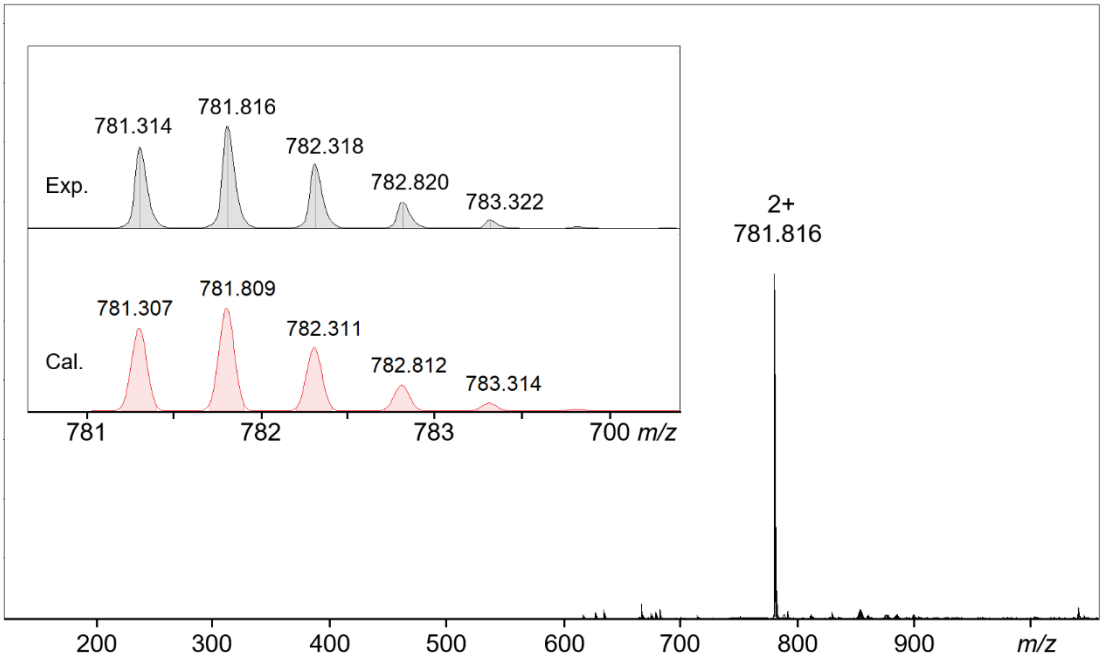

Figure S4. ESI-MS spectrum and experimental and calculated isotope patterns of ligand **L**.

Synthesis of complex **S**: To a mixed solvent of $CHCl_3$ (20 mL) and CH_3OH (15 mL) of ligand **L** (23.5 mg, 15.0 μmol), a solution of $Cd(NO_3)_2{\cdot}4H_2O$ (9.3 mg, 30.1 μmol) in CH_3OH (5.0 mL) was added. After being stirred at 65 °C for 12 h, excess NH_4PF_6 was added into the solution to precipitate the complex, which was filtered, washed with CH_3OH, and then dried *in vacuo*. The complex **S** was obtained as the pale-yellow solid in 93% yield (33.0 mg, 4.7 μmol). ^1H NMR (400 MHz, 298 K, CD_3CN, ppm): δ = 8.92 (s, 24H), 8.66 (d, J = 8.4 Hz, 24H), 8.32 (s, 12H), 8.05 (d, J = 7.6 Hz, 12H), 8.00-7.95 (m, 60H), 7.79 (dd, J = 12.2, 5.7 Hz, 36H), 7.44 (d, J = 8.3 Hz, 12H), 7.25-7.15 (m, 24H); ^{13}C NMR (126 MHz, 298 K, CD_3CN, ppm) δ = 155.58, 153.44, 150.03, 149.53, 148.66, 143.24, 141.28,

141.15, 141.05, 137.94, 137.42, 131.54, 130.23, 128.77, 127.06, 126.55, 126.25, 123.74, 122.36; ESI-MS (*m/z*): 1275.00 $[M\text{-}5PF_6^-]^{5+}$ (calcd. *m/z* = 1275.00), 1038.33 $[M\text{-}6PF_6^-]^{6+}$ (calcd. *m/z* = 1038.34), 869.30 $[M\text{-}7PF_6^-]^{7+}$ (calcd. *m/z* = 869.30), 742.51 $[M\text{-}8PF_6^-]^{8+}$ (calcd. *m/z* = 742.51), 643.80 $[M\text{-}9PF_6^-]^{9+}$ (calcd. *m/z* = 643.79), 565.02 $[M\text{-}10PF_6^-]^{10+}$ (calcd. *m/z* = 565.02).

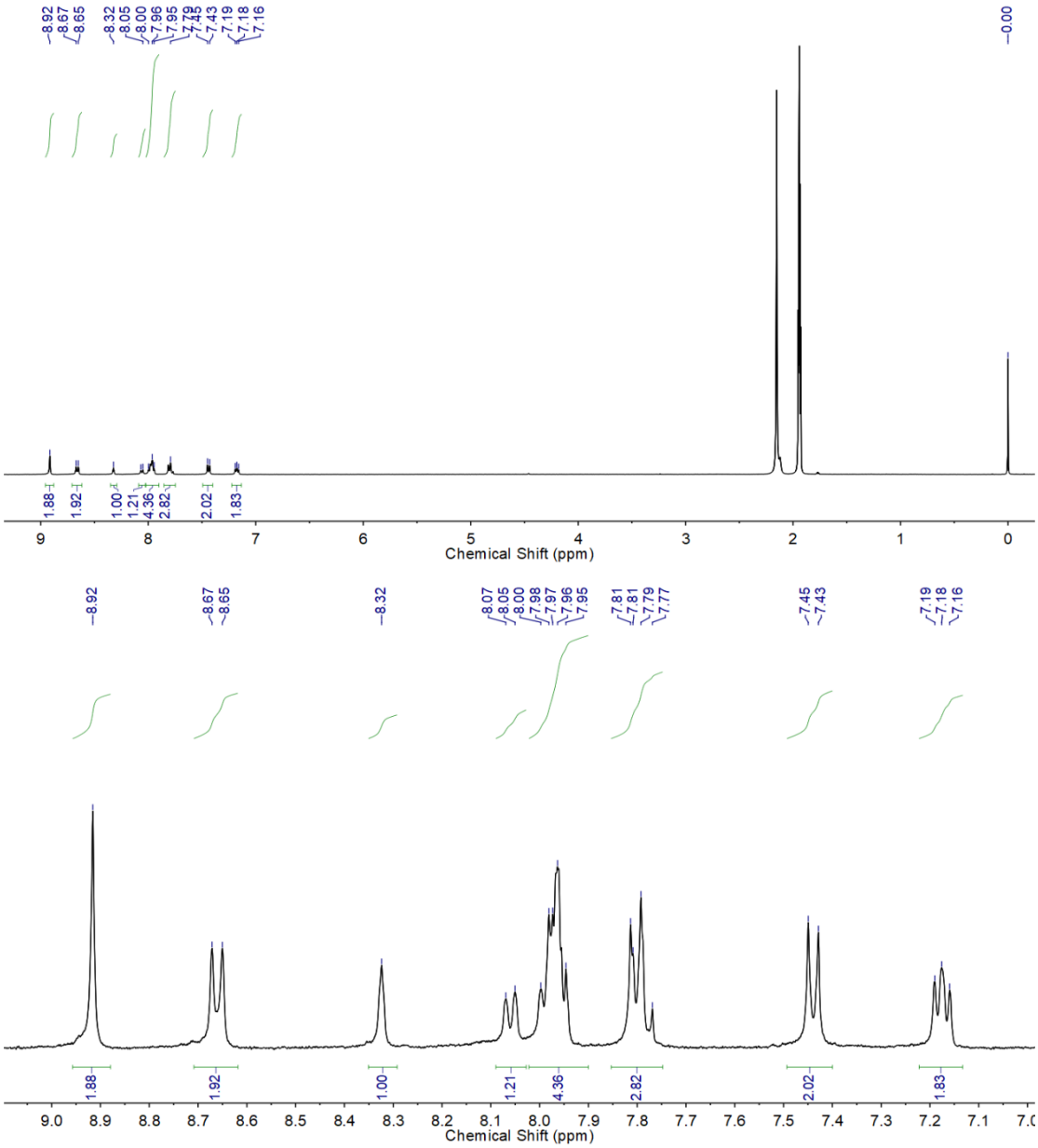

Figure S5. ^{1}H NMR spectrum of complex **S** in CD_3CN.

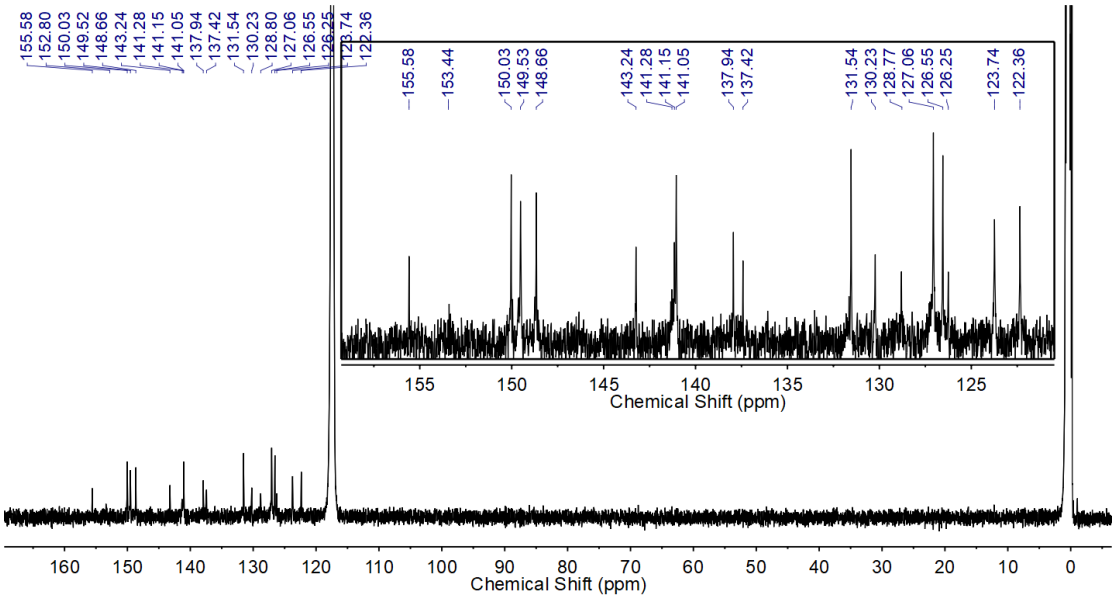

Figure S6. ^{13}C NMR spectrum of complex **S** in CD_3CN.

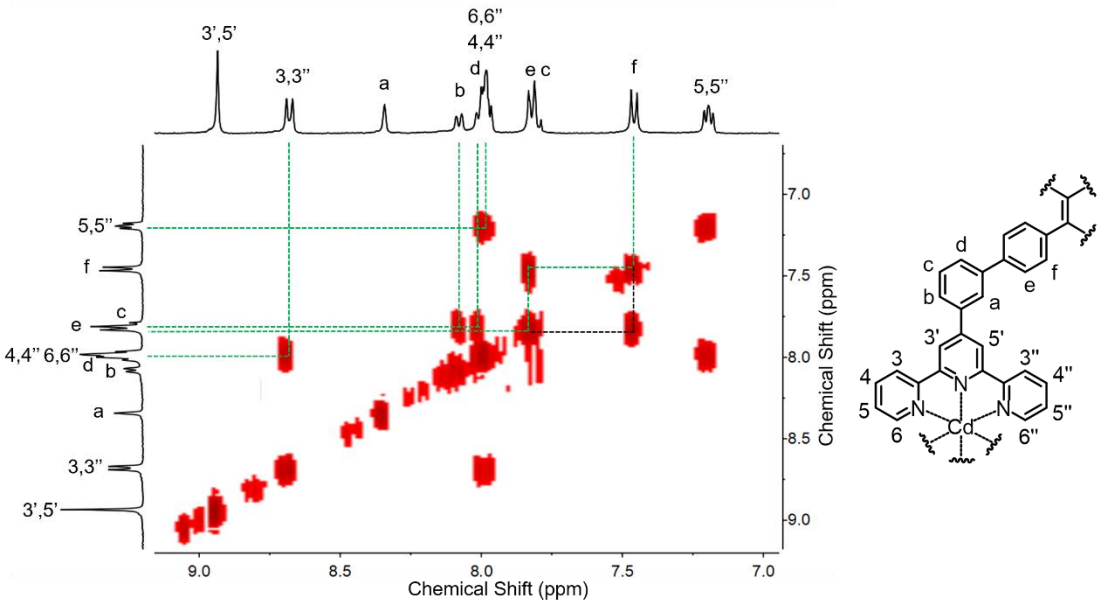

Figure S7. COSY spectrum of complex **S** in CD_3CN.

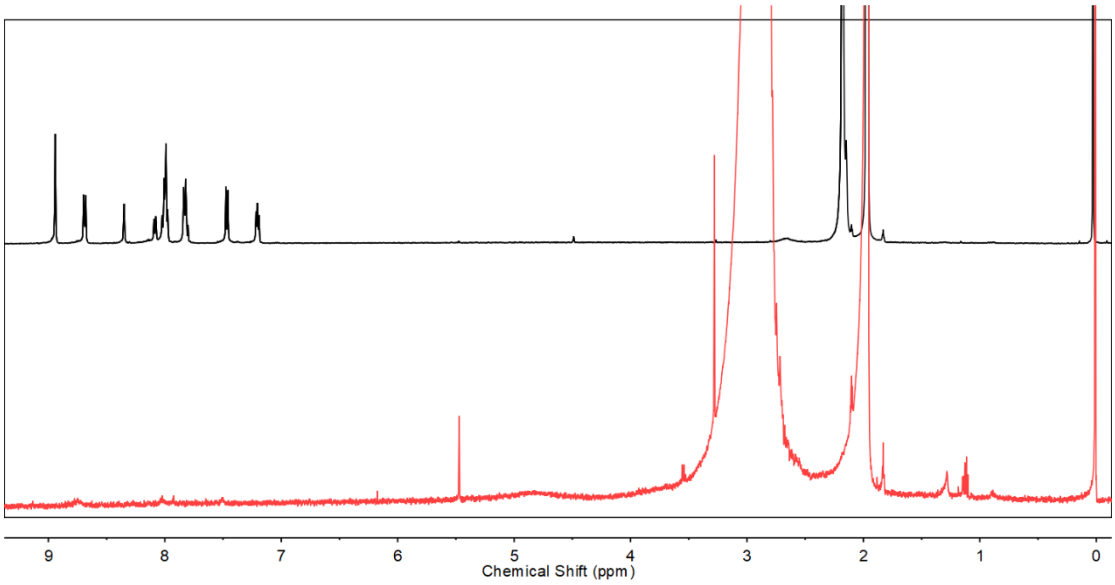

Figure S8. ^{1}H NMR spectra of complex **S** in CD_3CN (upper) and after 10 min upon the addition of 1 μmol Na_2S (down).

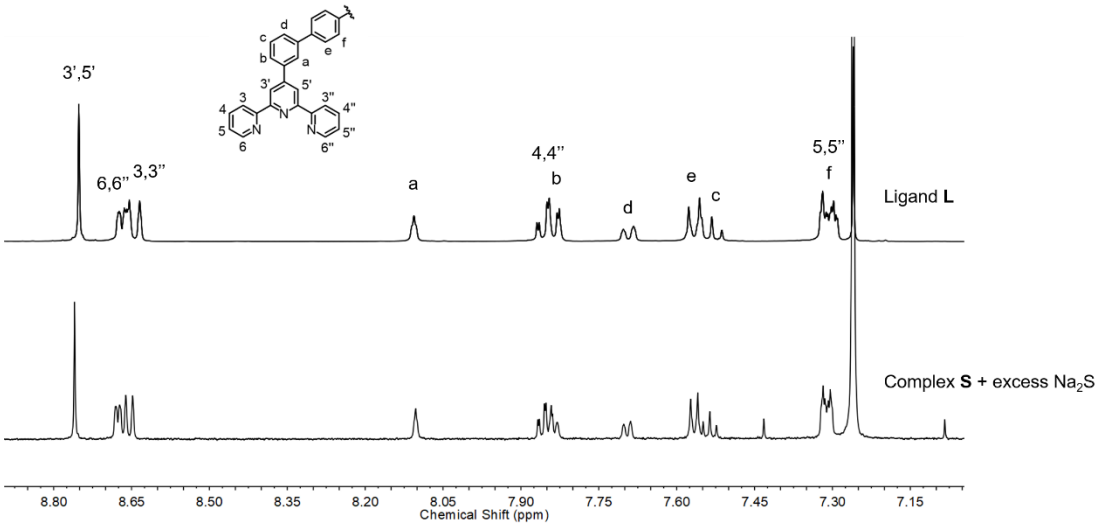

Figure S9. ^{1}H NMR spectra of ligand **L** in $CDCl_3$ (upper) and resultant solid products which were formed form complex **S** after 10 min upon the addition of 2 μmol Na_2S in CH_3CN/H_2O (down).

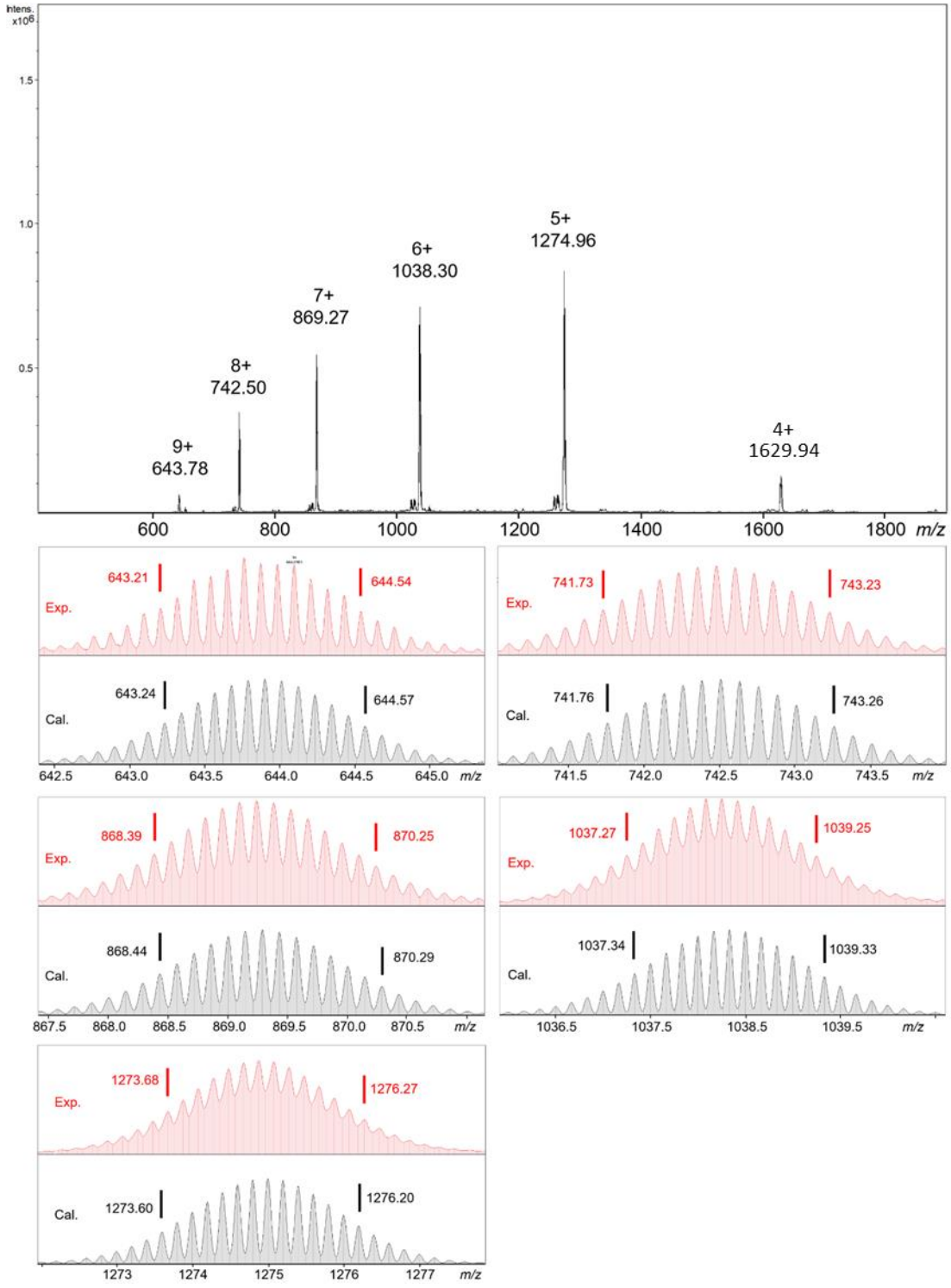

Figure S10. ESI-MS spectrum and experimental and calculated isotope patterns for the different charge states (5+ to 9+) of complex **S**.

Table S1. Experimental and calculated collision cross-sections of **S**.

Charge State	m/z	Exp. CCS(A^2)	Average CCS(A^2)	CacId. Average CCS(A^2)
6+	1038.1917	838.7904	808.9695 ± 20.2863	770.2948 ± 2.1663[a] 890.9943 ± 12.558[b]
7+	869.3006	812.8956		
8+	742.3955	803.1344		
9+	643.7997	782.4071		
10+	565.0234	807.6197		

The calculated values were obtained by [a] projection approximation (PA) and [b] trajectory method (TM) using MOBCAL

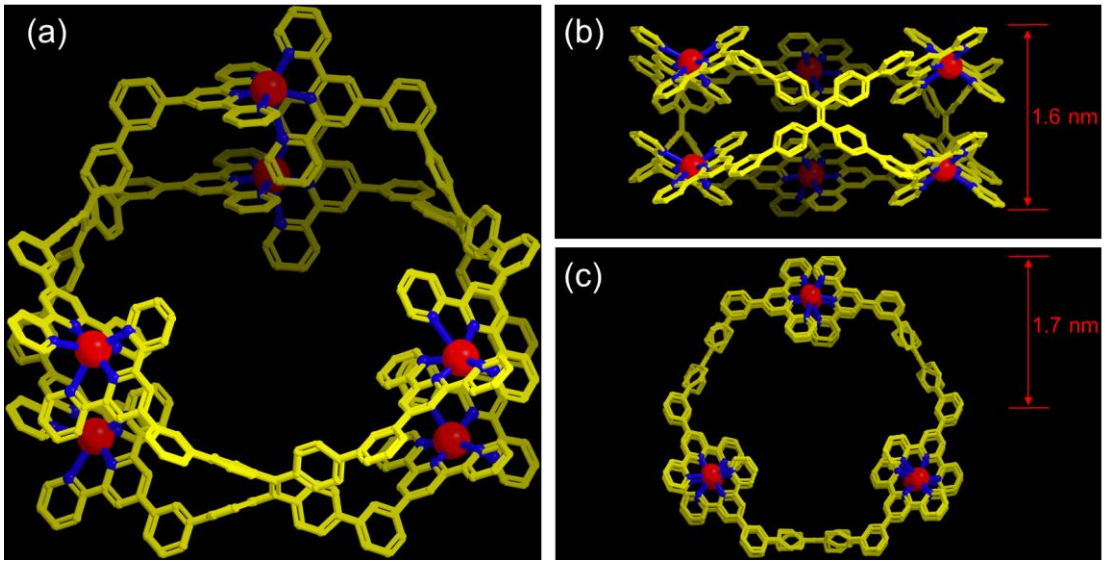

Figure S11. The energy-minimized structure (a) at the side sight (b) and at the top sight (c) from molecular modeling of complex **S**, the radius of nanobelt structure **S** was calculated to be 1.9 nm.

3. UV-vis and fluorescence spectra

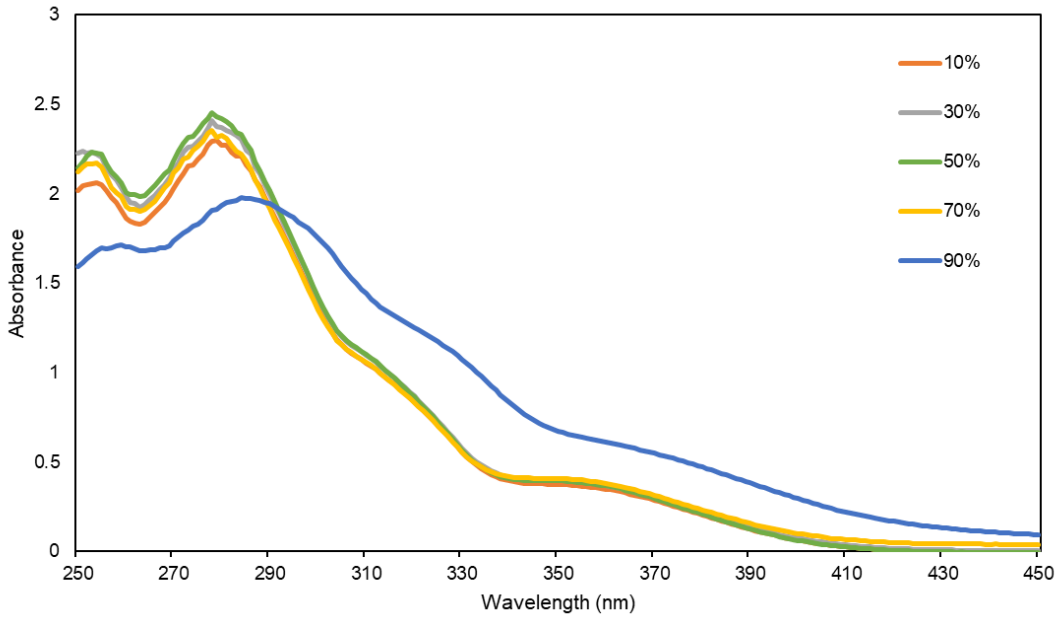

Figure S12. UV-vis spectra of ligand **L** in $CHCl_3$ with various hexane fractions at 298K (c = 1.6 × 10^{-5} M, 2 mL).

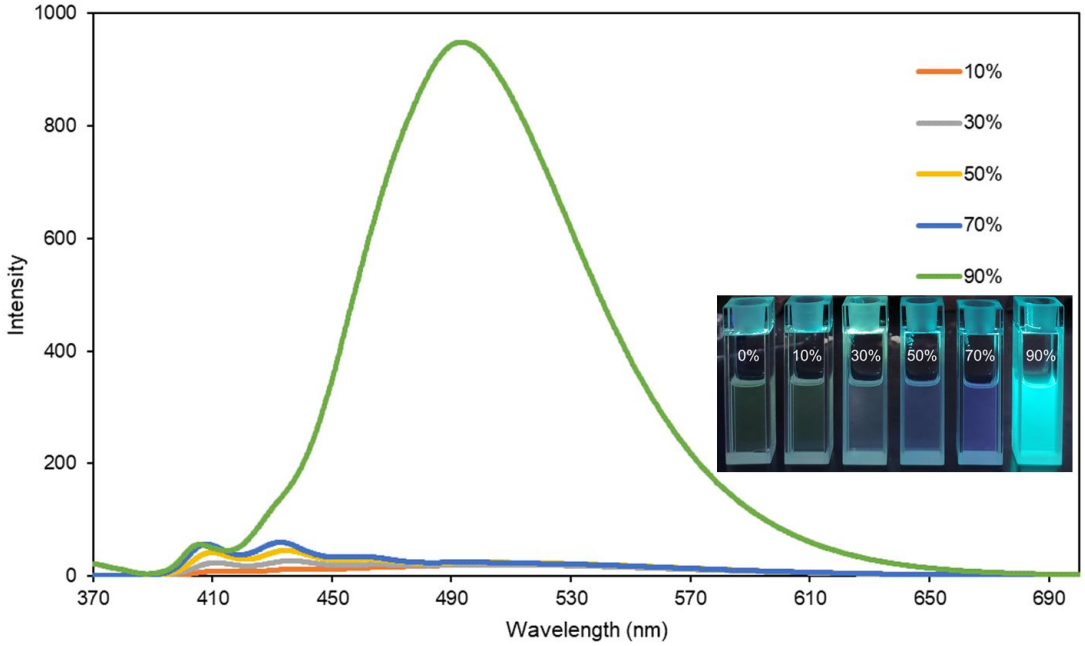

Figure S13. Fluorescence emission spectra (λ_{ex} = 360 nm; slit width: ex = 5 nm, em = 2.5 nm) and photographs upon (λ_{ex} = 365 nm) of ligand **L** in $CHCl_3$ with various hexane fractions at 298K (c = 1.6 × 10^{-5} M, 2 mL).

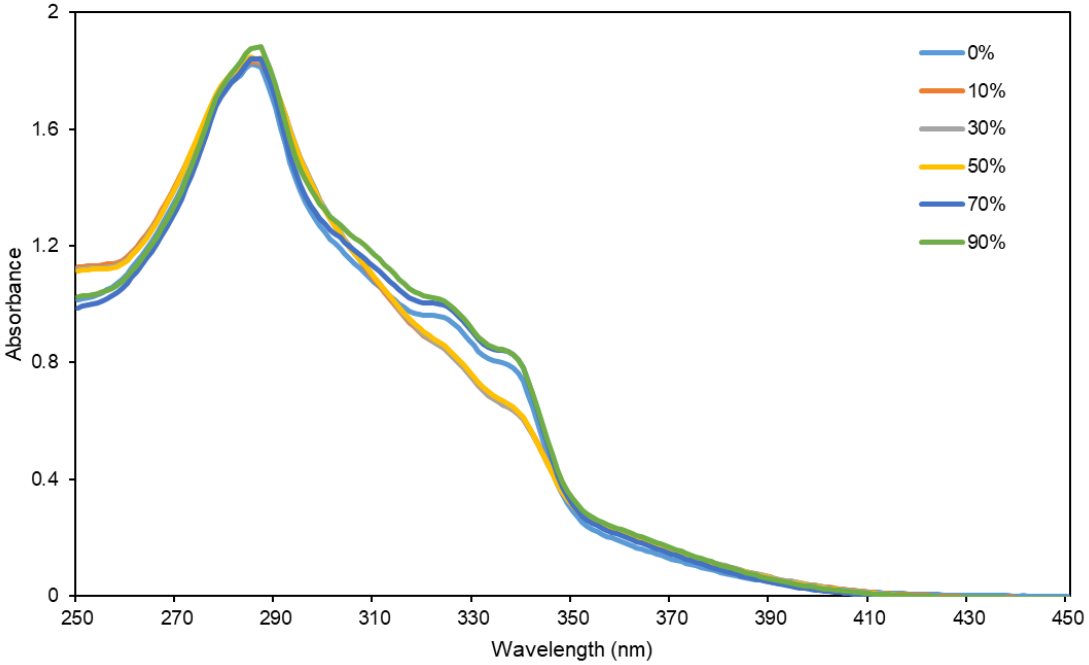

Figure S14. UV-vis spectra of complex **S** in CH_3CN with various CH_3OH fractions at 298K (c = 7.04×10^{-6} M, 2.0 mL).

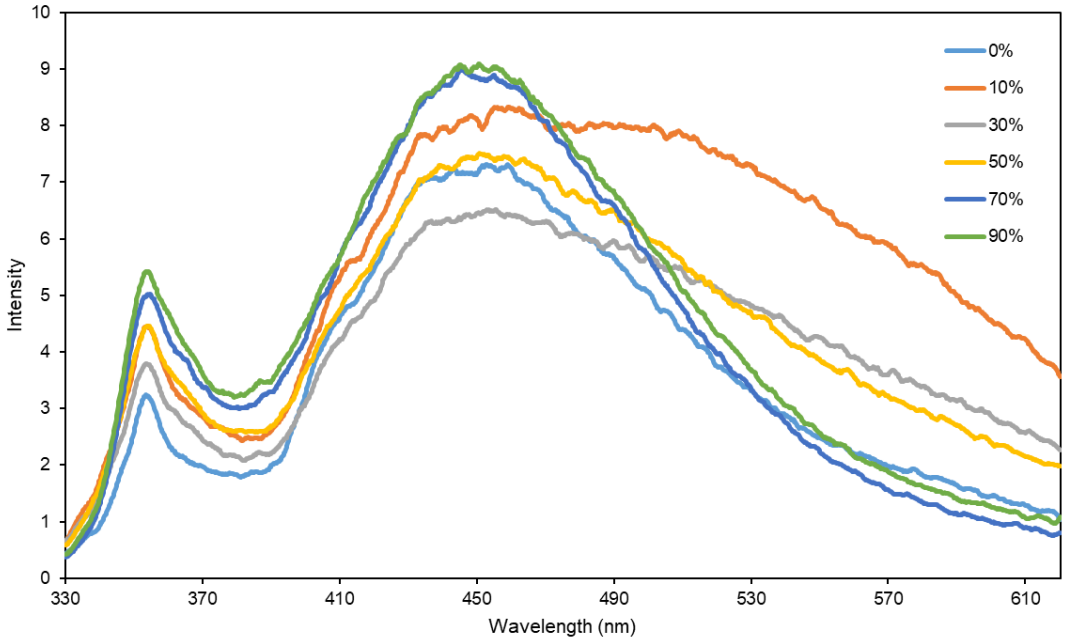

Figure S15. Fluorescence emission spectra (λ_{ex} = 320 nm; slit width: ex = 5 nm, em = 5 nm) of complex **S** in CH_3CN with various CH_3OH fractions at 298K (c = 7.04×10^{-6} M, 2.0 mL).

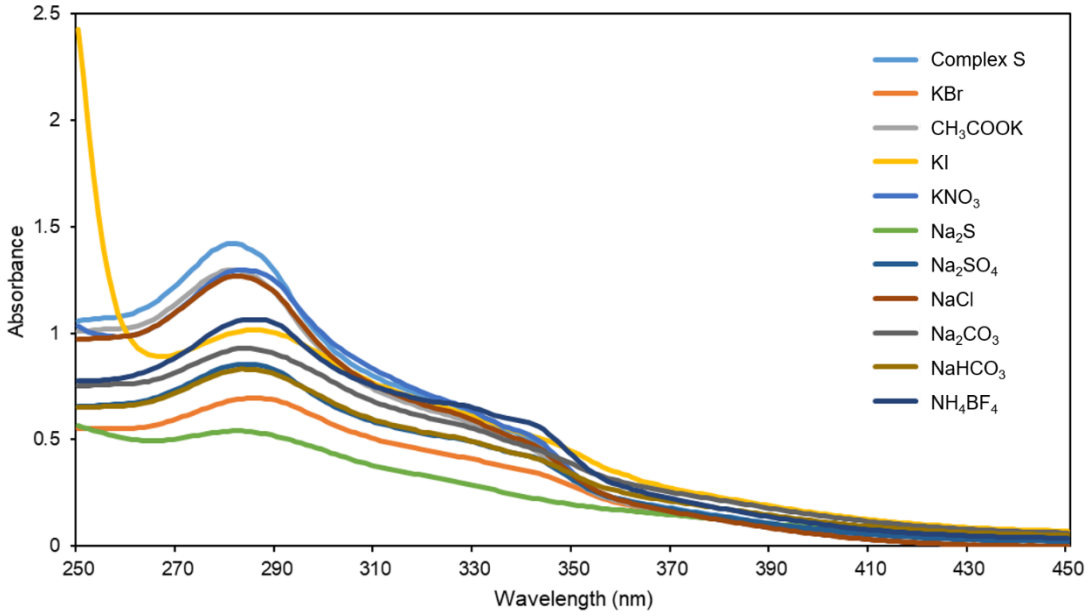

Figure S16. UV-vis spectra of complex **S** in 2.0 mL CH_3CN/H_2O mixtures (v/v, 1/9, c = 7.04×10^{-6} M) after and before addition of 4.0 μmol interfering species.

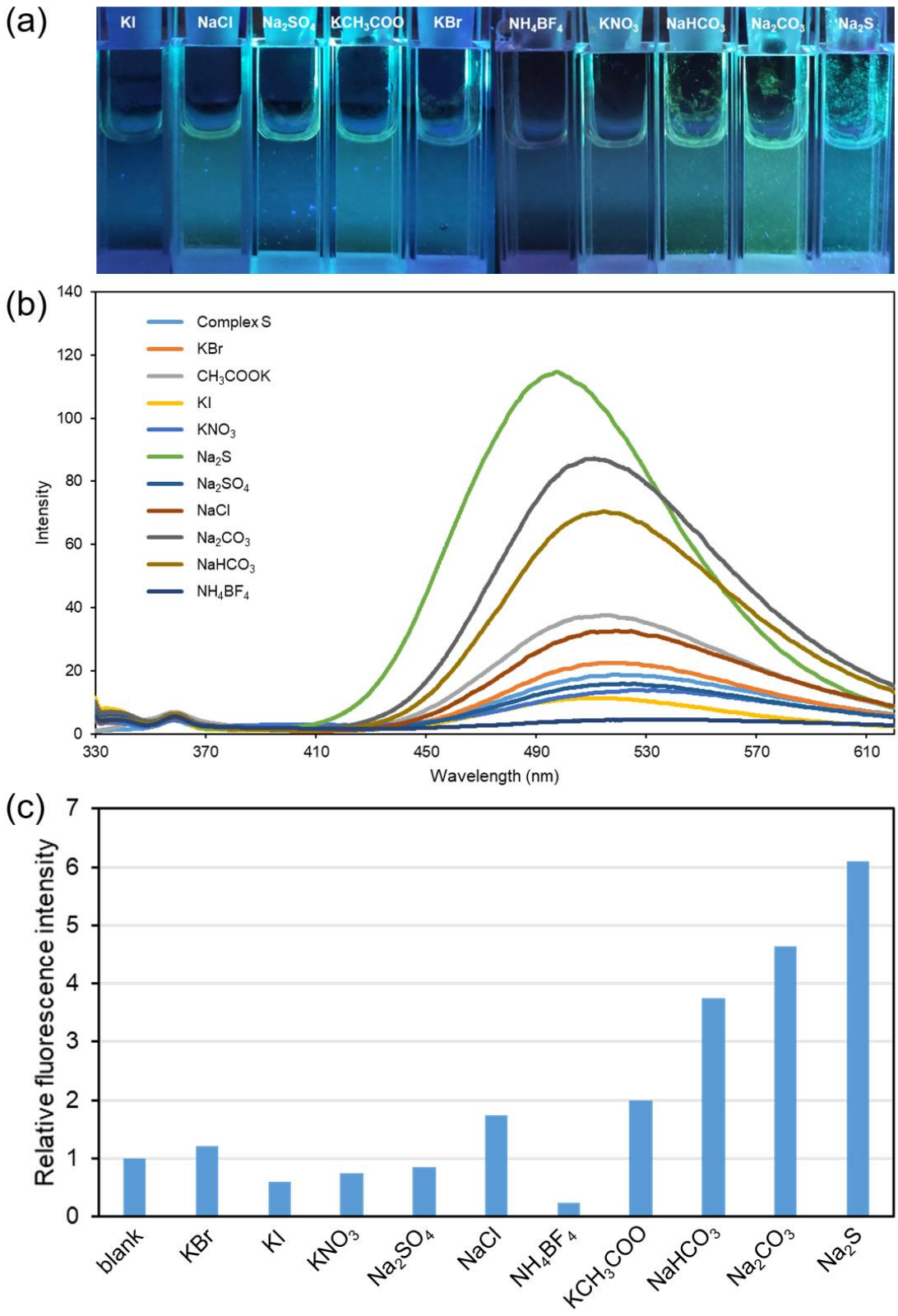

Figure S17. The fluorescence responses of complex **S** in 2.0 mL CH_3CN/H_2O at 298 K (v/v, 1/9, c = 7.04×10^{-6} M): (a) the photographs (λ_{ex} = 365 nm), (b) fluorescence spectra after adding 4.0 umol interfering species (λ_{ex} = 320 nm; slit width: ex = 5 nm, em = 5 nm) and (c) the relative fluorescence intensity of after and before addition of 4.0 umol interfering species.

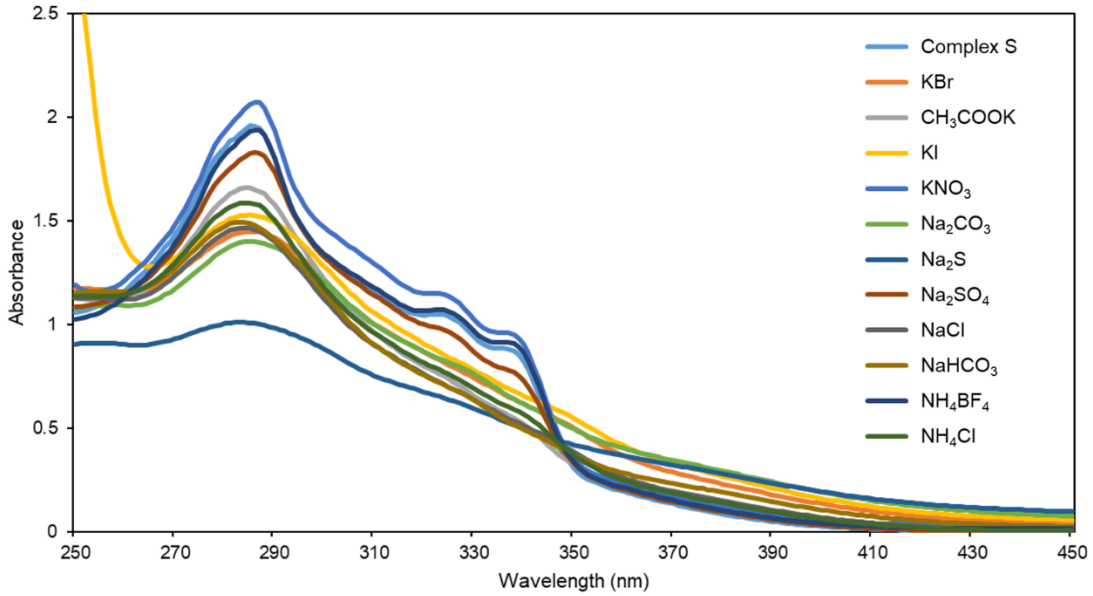

Figure S18. UV-vis spectra of complex **S** in 2.0 mL CH_3CN/H_2O mixtures (v/v, 1/1, c = 7.04×10^{-6} M) after 10 min after and before addition of 4.0 μmol interfering species.

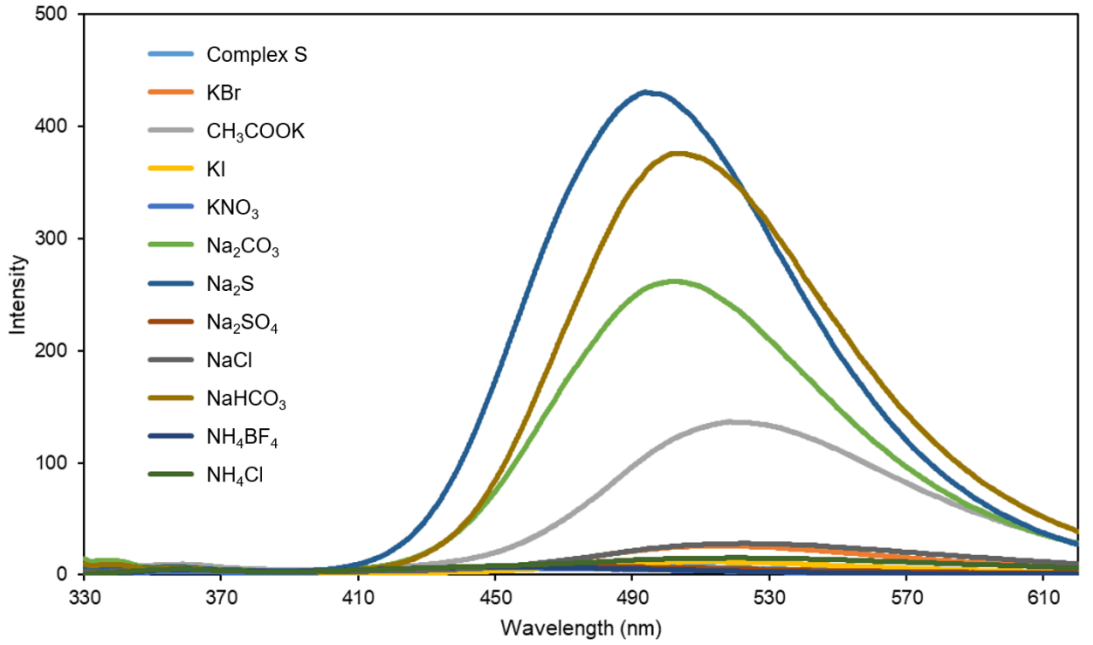

Figure S19. Fluorescence spectra of complex **S** in 2.0 mL CH_3CN/H_2O mixtures (v/v, 1/1, c = 7.04×10^{-6} M) after and before addition of 4.0 μmol interfering species. (λ_{ex} = 320 nm; slit width: ex = 5 nm, em = 5 nm)

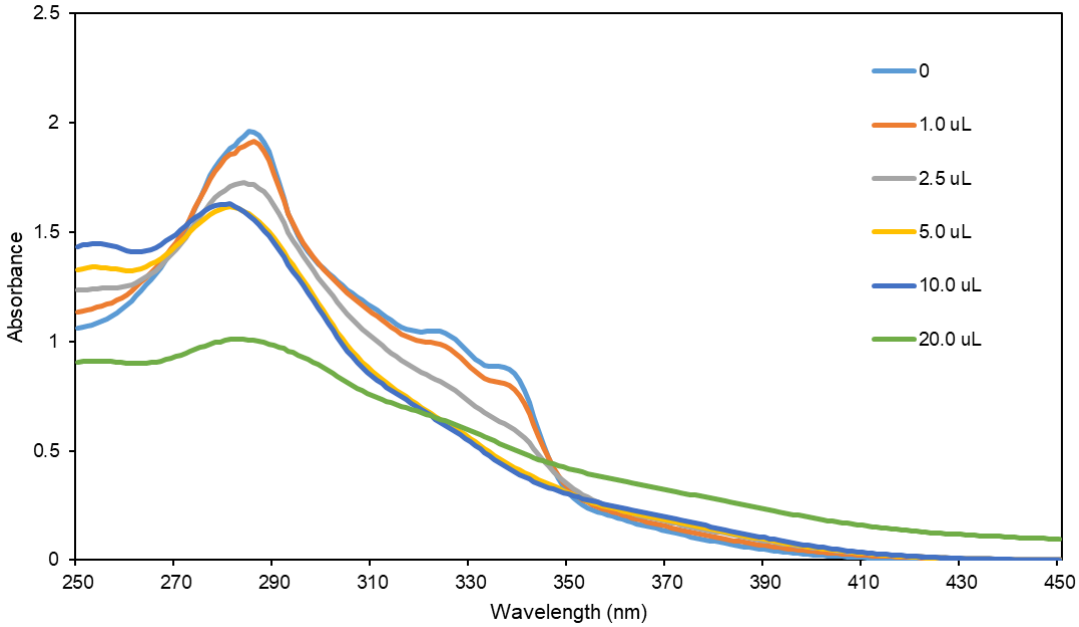

Figure S20. UV-vis spectra of complex **S** in 2.0 mL CH_3CN/H_2O mixtures (v/v, 1/1, c = 7.04×10^{-6} M) after 10 min upon the addition of increasing concentrations of Na_2S.

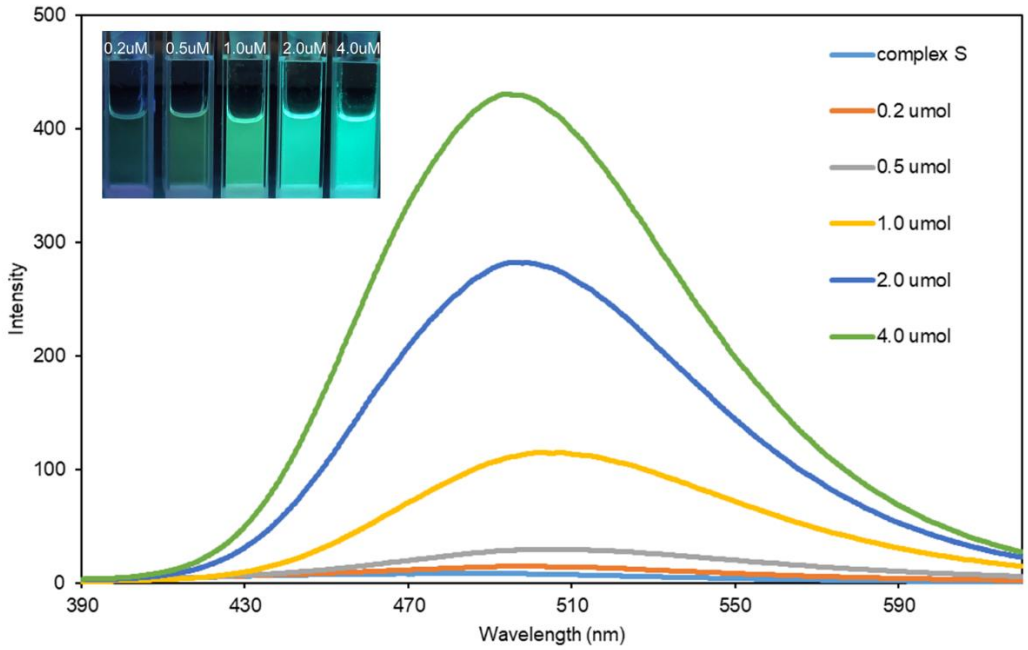

Figure S21. Fluorescence spectra (λ_{ex} = 320 nm; slit width: ex = 5 nm, em = 5 nm) and photographs (λ_{ex} = 365 nm) of complex **S** in 2.0 mL CH_3CN/H_2O mixtures (v/v, 1/1, c = 7.04×10^{-6} M) after 10 min upon the addition of increasing concentrations of Na_2S.

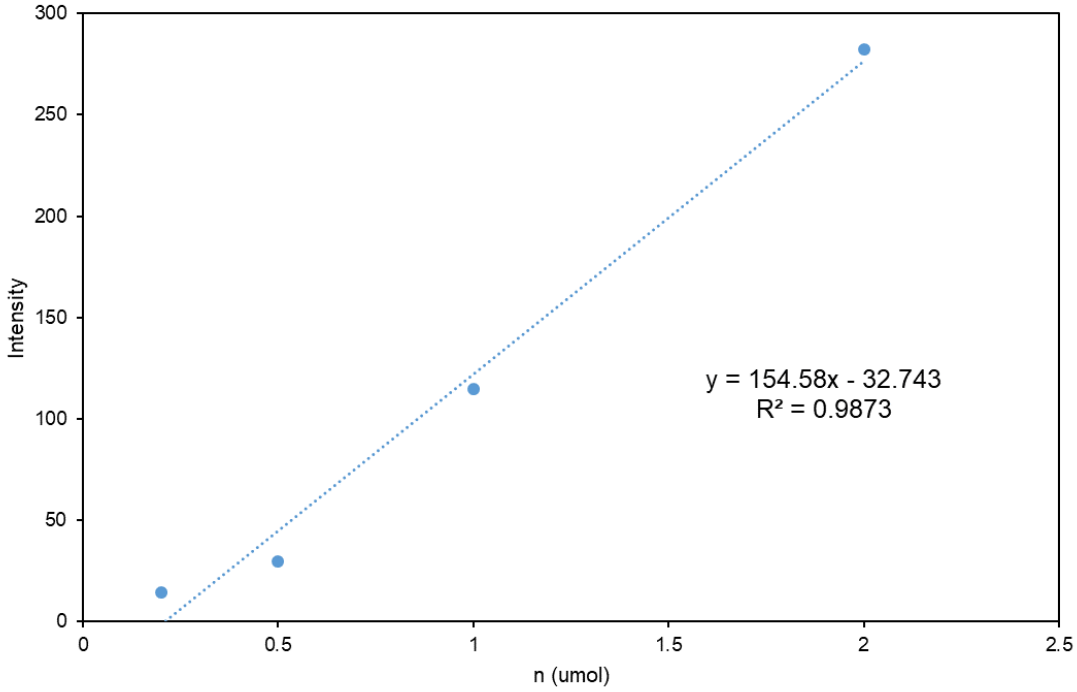

Figure S22. The emission intensities of complex **S** in 2.0 mL CH_3CN/H_2O mixtures (v/v, 1/1, c = 7.04×10^{-6} M) at 494 nm as a function of Na_2S concentration.

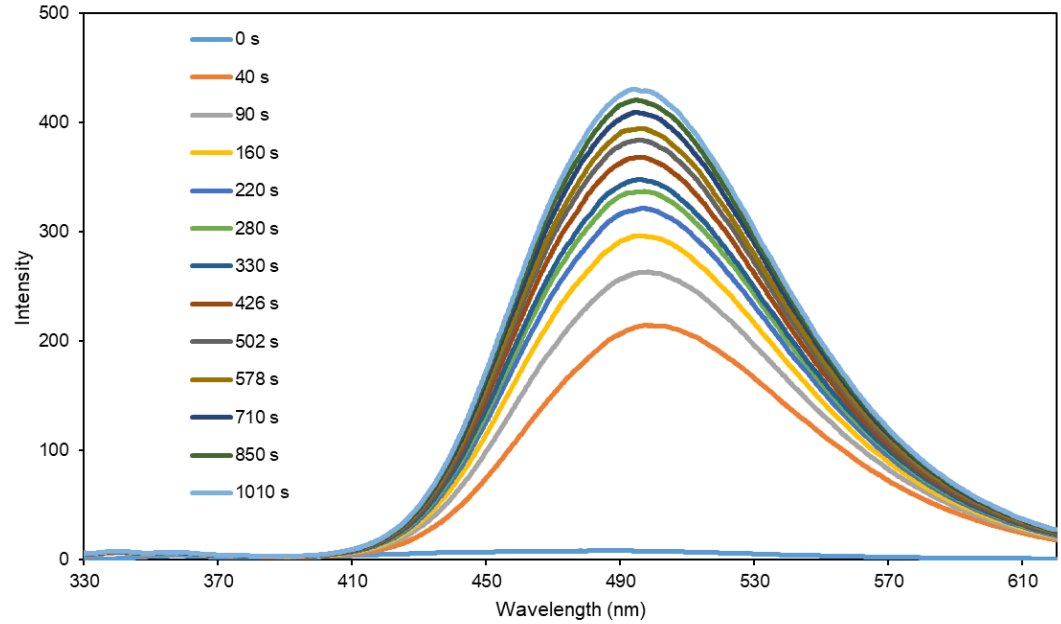

Figure S23. The time dependent fluorescence spectra of complex **S** in 2.0 mL CH_3CN/H_2O mixtures (v/v, 1/1, c = 7.04×10^{-6} M) after addition of 4.0 μmol Na_2S. (λ_{ex} = 320 nm; slit width: ex = 5 nm, em = 5 nm)

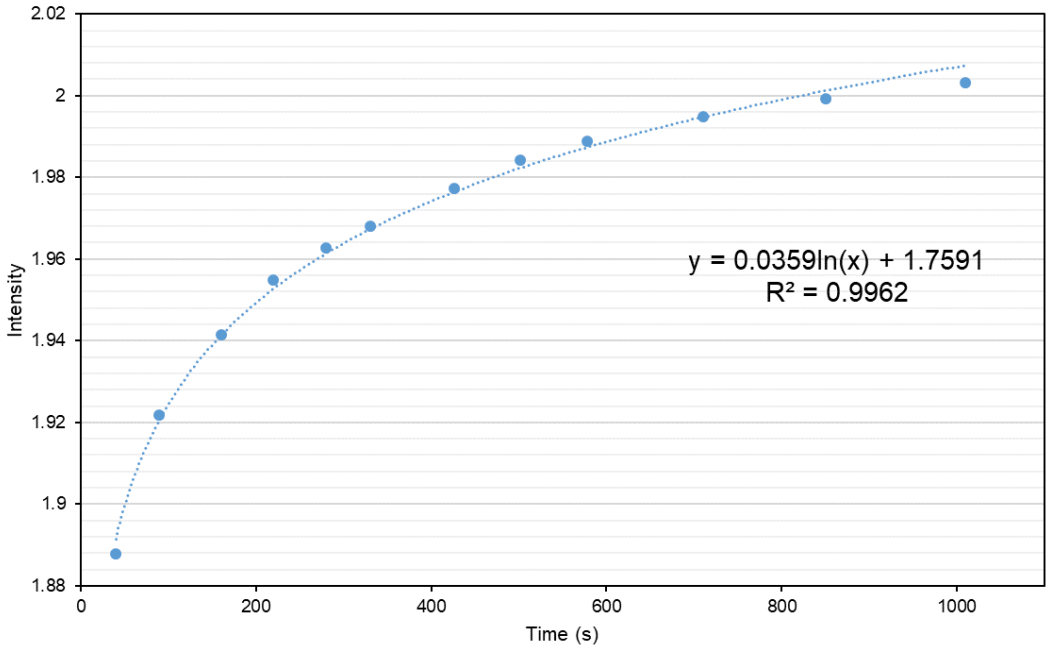

Figure S24. The fluorescence intensity at 494 nm of complex **S** in CH_3CN/H_2O mixtures (v/v, 1/1, c = 7.04×10^{-6} M) after addition of 4.0 μmol Na_2S as a function of time.

4. Reference

S1. a) K. B. Shelimov, D. E. Clemmer, R. R. Hudgins, M. F. Jarrold, *J. Am. Chem. Soc.*, **1997**, *119*, 2240-2248; b) S. J. Valentine, J. G. Anderson, A. D. Ellington, D. E. Clemmer, *J. Phys. Chem. B*, **1997**, *101*, 3891-3900; c) I. Campuzano, M. F. Bush, C. V. Robinson, C. Beaumont, K. Richardson, H. Kim, H. I. Kim, *Anal. Chem.*, **2012**, *84*, 1026-1033; d) M. F. Bush, I. D. G. Campuzano, C. V. Robinson, *Anal. Chem.*, **2012**, *84*, 7124-7130; e) R. Salbo, M. F. Bush, H. Naver, I. Campuzano, C. V. Robinson, I. Pettersson, T. J. D. Jørgensen, K. F. Haselmann, *Rapid Comm. Mass Spectrom.*, **2012**, *26*, 1181-1193.

S2. W. Yang, G. Chang, H. Wang, T. Hu, Z. ao, K. Alfooty, S. Xiang, B. Chen, Eur. *J. Inorg. Chem.*, **2016**, *2016*, 4470-4475.